



# Multistability and memory effect in a highly turbulent flow: experimental evidence for a global bifurcation

Florent Ravelet, Louis Marié, Arnaud Chiffaudel, François Daviaud

## ► To cite this version:

Florent Ravelet, Louis Marié, Arnaud Chiffaudel, François Daviaud. Multistability and memory effect in a highly turbulent flow: experimental evidence for a global bifurcation. *Physical Review Letters*, 2004, 93, pp.164501. 10.1103/PhysRevLett.93.164501 . hal-00002925

**HAL Id: hal-00002925**

**<https://hal.science/hal-00002925>**

Submitted on 21 Sep 2004

**HAL** is a multi-disciplinary open access archive for the deposit and dissemination of scientific research documents, whether they are published or not. The documents may come from teaching and research institutions in France or abroad, or from public or private research centers.

L'archive ouverte pluridisciplinaire **HAL**, est destinée au dépôt et à la diffusion de documents scientifiques de niveau recherche, publiés ou non, émanant des établissements d'enseignement et de recherche français ou étrangers, des laboratoires publics ou privés.

# Multistability and memory effect in a highly turbulent flow: Experimental evidence for a global bifurcation

Florent Ravelet, Louis Marié, Arnaud Chiffaudel,\* and François Daviaud

*Service de Physique de l'État Condensé, DSM, CEA Saclay, CNRS URA 2464, 91191 Gif-sur-Yvette, France*

(Submitted to Phys. Rev. Lett. 19 May 2004)

We report an experimental evidence of a global bifurcation on a highly turbulent von Kármán flow. The mean flow presents multiple solutions: the canonical symmetric solution becomes marginally unstable towards a flow which breaks the basic symmetry of the driving apparatus even at very large Reynolds number. The global bifurcation between these states is highly subcritical and the system thus keeps a memory of its history. The transition recalls low-dimension dynamical systems transitions and exhibits a very peculiar statistics. We discuss the role of turbulence in two ways: the multiplicity of hydrodynamical solutions and the effect of fluctuations on the nature of transitions.

PACS numbers: 05.45.-a, 47.20.-k, 47.27.Sd

Non-linear systems generally present multiple solutions and various transitions between them. Moreover, stability and transitions are influenced by the presence of noise and/or fluctuations. In the field of turbulence, the question of multistability of turbulent flows, for example in tornadoes [1, 2], delta wing flow [3], wakes [4], and vortex breakdown [5], remains open and unsolved. While multiple analytical or numerical solutions are often encountered for the Navier-Stokes equation at even moderate Reynolds number (e.g., for swirling flows [2, 5, 6, 7, 8]), these solutions are generally neither experimentally relevant, nor stable at very high Reynolds number. Furthermore, turbulent flows at very high Reynolds number are generally expected to statistically respect the basic symmetries of their driving apparatus. Indeed, even if bifurcations and symmetry breaks occur on the way to turbulence, the fully developed turbulent state is known to restore the broken symmetries, in the limit of infinite Reynolds number and far from boundaries [9]. In this Letter, we experimentally study the multistability of a turbulent von Kármán flow between two counter-rotating disks in a finite vessel at very high Reynolds number. This system undergoes a subcritical global bifurcation between turbulent states characterized by mean flows of different topology and symmetry. These turbulent states coexist at high Reynolds number and can be “prepared” specifically, i.e., they keep a memory of the system history. Since these states are highly fluctuating turbulent states, we also address the question of the role of the fluctuations for such a transition. Actually, the effect of an external noise on an existing transition is well documented [10], but the global bifurcation reported here does only take place over an already fluctuating turbulent regime. Do fluctuations trigger the bifurcation as multiplicative noise do for nonlinear oscillators [11] and turbulent  $\alpha$ -effect do for dynamo action [12] ?

*Experimental setup.* We call von Kármán type flow the flow generated between two coaxial counter-rotating impellers in a cylindrical vessel. The cylinder radius and height are respectively  $R = 100$  mm and  $H_c = 500$  mm.

We use bladed disks to ensure inertial stirring. Most of the inertially driven von Kármán setups studied in the past dealt with straight blades [13, 14]. In this Letter, the impellers consist of 185 mm diameter disks each fitted with 16 curved blades —curvature radius 50 mm, height 20 mm (Fig. 1). The distance between the inner faces of the disks is  $H = 180$  mm which defines a working space for the flow of aspect ratio  $H/R = 1.8$ . With curved blades, the directions of rotation are no longer equivalent. We rotate the impellers clockwise (with the concave face of the blades). Four baffles ( $10 \times 10 \times 125$  mm) can be added along the cylinder wall.

The impellers are driven by two independent brushless 1.8 kW motors, with a speed servo loop control. The motor rotation frequencies  $f_1, f_2$  can be varied independently in the range 0–15 Hz. An experiment is thus characterized by two numbers:  $f = \sqrt{(f_1^2 + f_2^2)}/2$  measuring the intensity of the forcing and  $\theta = (f_2 - f_1)/(f_1 + f_2)$  measuring the speed dissymmetry ( $-1 \leq \theta \leq 1$ ). For exact counter rotation  $f_1 = f_2 = f$  and  $\theta = 0$ . The speed servo loop control ensures a precision of 0.5% on  $f$ , and an absolute precision of  $\pm 0.002$  on  $\theta$  for small values.

The working fluid is water. Copper cooling coils behind the impellers and a thermoregulated bath ensure a thermal regulation with a precision of 1°C. Velocity fields are measured by Laser Doppler Velocimetry (LDV). Torques are measured as an image of the current consumption in the motors given by the servo drives and have been calibrated by calorimetry. The analog signal is low-pass filtered at 10 Hz. For a typical frequency  $f = 4$  Hz at 35°C, the integral Reynolds number is  $Re = 2\pi f R^2 \nu^{-1} \simeq 3 \cdot 10^5$  and the velocity fluctuation

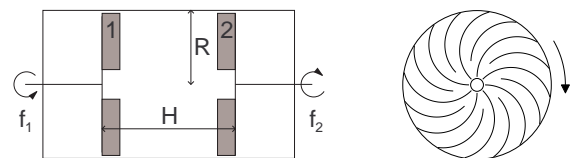


FIG. 1: Sketch of the experimental setup and of the impellers blades profile. The arrow indicates the positive rotation sense.

level is of order 30%: the flow is highly turbulent.

The von Kármán flow phenomenology is the following. Each impeller acts as a centrifugal pump: the fluid rotates with the impeller and is expelled radially. It is pumped in the center of the impeller. In the exact counter-rotating regime, the flow is divided into two toric cells separated by an azimuthal shear layer. The problem (equation and boundary conditions) is invariant under rotations of  $\pi$  ( $\mathcal{R}_\pi$ ) around any radial axis passing through the center of the cylinder. The velocity field is expected  $\mathcal{R}_\pi$ -invariant.

A “statistical” symmetry breaking. In our high Reynolds number regime, the flow is highly turbulent. For instance the *rms* value of the velocity is of the same order of magnitude as the mean value. In Fig. 2 (left), we present a map of the mean part of the exact counter-rotation flow measured by LDV. Two cells are observed, the flow is  $\mathcal{R}_\pi$ -invariant: the symmetries are statistically restored [9]. The mean angular momentum of the fluid is equal to zero: the two impellers produce the same mean torque to maintain the flow. This situation is well-known and documented. We label this symmetric state (*s*).

However, with our curved blades, we observe for small  $\theta$  a global bifurcation of the flow after a certain time  $t_{bif}$ : both mean velocity field and torques display dramatic changes (Fig. 3). The two torques are suddenly 4 times larger, and are no longer equal. The mean flow exhibits only one cell (Fig. 2, right). In the bulk, the fluid is pumped toward impeller 1 without rotation. Then the fluid is expelled radially and starts spiraling along the cylinder until it meets impeller 2 which rotates in the opposite direction. It is abruptly stopped and reinjected near the axis. We label this state ( $b_1$ ). A third state ( $b_2$ ) is deduced from ( $b_1$ ) by exchanging the roles of impellers 1 and 2. In bifurcated states ( $b_1$ ) or ( $b_2$ ), the fluid is globally in rotation: the mean angular momentum is not zero.

Finally, three states are observed: the canonical  $\mathcal{R}_\pi$ -

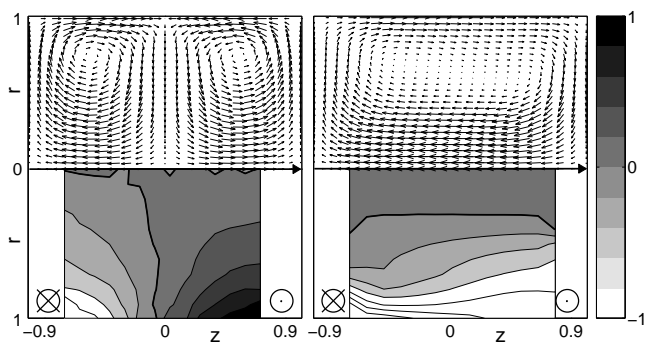


FIG. 2: Dimensionless mean velocity field measured at  $\theta = 0$  by LDV over 120 integral turn-over time by grid point to ensure good convergence;  $f = 2$  Hz ( $Re = 1.5 \cdot 10^5$ ). Left: symmetric state (*s*). Right: bifurcated state ( $b_1$ ). Space coordinates in units of  $R$ . Gray code stands for azimuthal velocity. Isolines are distant of 0.2 and the gray code saturates in the right map. Bold lines indicate level zero.

invariant—in a statistical sense—state (*s*) and two bifurcated states which break the  $\mathcal{R}_\pi$  symmetry at  $\theta = 0$ , but are images one of the other by  $\mathcal{R}_\pi$ . We detail in the next section the transitions between these different states.

*Hysteresis loops.* The difference between the two torques characterizes the different states. We have checked that, as expected for so high a Reynolds number [9], the torque  $T$  given by one impeller for a given  $(f, \theta)$  does not depend on  $Re$  and scales as:  $T(f, \theta) = K_p(\theta) \rho R^5 (2\pi f)^2$  [14], with  $\rho$  the fluid density and  $K_p$  a dimensionless power coefficient.

In Fig. 4, we plot the dimensionless difference  $\Delta K_p$  between the two torques *vs.*  $\theta$  for several configurations. For straight blades, we observe a continuous curve from  $\theta = -1$  to  $\theta = 1$  (Fig. 4a) with two transitions between one- and two-cells flows at  $\theta = \pm 0.13$ . For impellers with curved blades and no baffles on the cylinder wall, we observe the three states in Fig. 4b. For  $\theta = 0$ , we recognize state (*s*) ( $\Delta K_p = 0$ ), and both bifurcated states ( $b_1$ ) and ( $b_2$ ). State (*s*) branch is almost reduced to one point and can only be reached by starting the two motors simultaneously. Its stability is discussed in the next section. The bifurcated state ( $b_1$ ) lies on a branch coming continuously from  $\theta = -1$  ( $f_2 = 0$ ). Starting from  $\theta = -1$  and increasing  $\theta$ , we stay on the ( $b_1$ ) branch even for  $\theta > 0$ : impeller 1 keeps rotating and pumping the fluid although its rotation rate is weaker than impeller 2 rotation rate. For  $\theta \simeq 0.16$  there is a transition from ( $b_1$ ) to ( $b_2$ ): the fluid abruptly changes its sense of rotation. There is a large hysteric cycle. Note that it is impossible to reach the symmetric state (*s*) by this way. The global quantities of this highly turbulent flow keep memory of the way the system has been started from rest. An intermediate situation is reached with the same curved blades and baffles on the wall (Fig. 4c). Baffles break the spiraling flow along the wall of the cylinder, which is a major feature of the bifurcated state velocity field. The hysteric cycle splits into two classical first order cycles: the central symmetric state becomes stable and can be obtained from any initial condition.

*Stability of the central branch (s).* We focus now on the transition from symmetric state to bifurcated state for curved blades without baffles. As mentioned before,

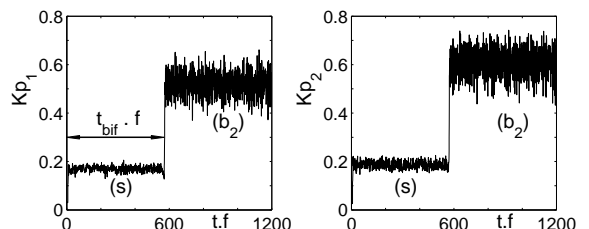


FIG. 3: Time series of dimensionless torque showing the bifurcation (*s*)  $\rightarrow$  ( $b_2$ ), for  $\theta = 0.0204$ ,  $f = 4.08$  Hz. Left: torque on impeller 1. Right: torque on impeller 2. The bifurcation time is the time when the torque on impeller 1 reaches 140% of the mean value for the symmetric state (*s*).

the central branch is very small and, for a given  $(f, \theta)$ , the transition occurs after a certain time  $t_{bif}$  which exhibits a complex statistics.

So we performed the following experiments: starting from rest, we simultaneously start both motors to a given  $(f, \theta)$  with a short ramp (typically 1 s) and record the torques. Few seconds after the instant  $t_{bif}$  when bifurcation occurs, we stop the motors, wait a minute and run again. We perform typically 500 runs to get the distribution of bifurcation times. The cumulative distribution function (CDF) for  $t_{bif}$  (Fig. 5) shows exponential behavior for the probability of staying in the symmetric state a time greater than  $t$ :  $P(t_{bif} > t) = A \exp[-(t - t_0)/\tau]$ ,  $t_0$  is characteristic of the transition duration ( $t_0 \cdot f \sim 5$ ). Thus, we obtain a characteristic bifurcation time  $\tau(f, \theta)$  by non-linear fitting of the CDF. We performed the experiment for three values of  $f$ . The results are shown in Fig. 6 in log-log scale. There is no noticeable dependence on  $f$  and  $\tau$  behaves as  $|\theta|^{-6}$ . So, as  $\theta$  tends to zero,  $\tau$  diverges very fast to infinity: the central point is marginally stable. The physical phenomenon at the origin of such an exponent remains to be understood.

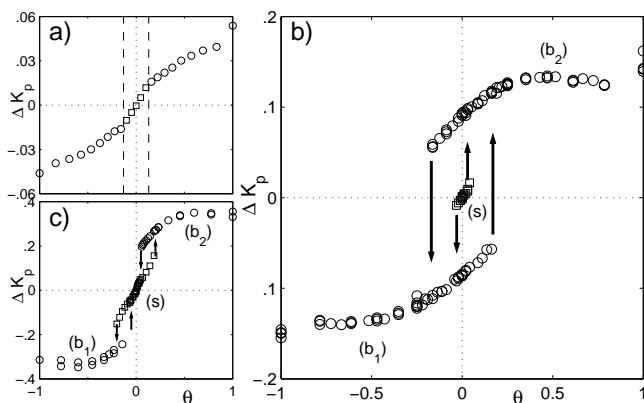


FIG. 4: Dimensionless torque difference  $\Delta K_p$  vs.  $\theta$  for  $Re$  in the range  $2 - 8 \times 10^5$ . Straight blades (a) exhibit continuous transition from 1-cell flow to 2-cells flow for  $\theta = \pm 0.13$  (vertical lines). Curved blades without (b) or with (c) baffles along cylinder wall show subcritical transitions between symmetric/2-cells (s)-(□) and bifurcated/1-cell ( $b_1$ )-(b<sub>2</sub>) states (○).

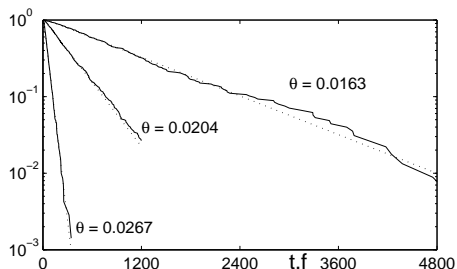


FIG. 5: Cumulative density function of bifurcation times for three different  $\theta$  at  $f = 4.16$  Hz. Dotted line: non-linear exponential fit.

*Discussion.* The experiment presented here opens mainly two problems: (i) the existence and the nature of multiple regimes for this turbulent flow, and (ii) the role of the noise or the fluctuations in some transitions between these flow regimes, i.e., the stability problem for the two-cell (s) branch.

We first try to explain the existence of multiple stable regimes by hydrodynamical basic arguments. The von Kármán (VK) class of Navier-Stokes solutions in semi-infinite space with one or two infinite rotating disks for end-conditions has been extensively studied since 1921 [6, 7, 15]. Experiments are necessarily limited in diameter and do not strictly belong to the same class. However the approximation is very commonly made at least for small  $H/R$ . In practice, in our system, and in the spirit of Batchelor [6] and Stewartson [7], we construct finite-aspect-ratio solutions of our experimental VK problem at high  $Re$  (Fig. 2) with (i) any typical truncated Batchelor [6] solution for  $0 \leq r \lesssim R/2$  together with (ii) some recirculation flow in rotation in  $R/2 \lesssim r \lesssim R$  and (iii) a thin boundary layer near the outer cylinder which matches this rotation [16]. The two-cell mean flow (s) is simply described in the laboratory frame by two rotating regions inertially driven by the blades and separated by a shear layer near mid-height. Both disks centrifugally expel the fluid. Let's now consider one-cell flows ( $b_1$ ) and ( $b_2$ ). Since one disk expels the fluid and the other reinjects it to the center, these flows resemble the corotating ( $f_1, f_2 < 0$ ) regime solutions [6, 7] characterized by: uniform rotation of the bulk; a boundary layer on each disk; pumping from one disk to the other and recirculation at infinity. This solution has no shear layer. Let's note that mean bulk rotation—for  $r \lesssim R/2$ —is close to zero (Fig. 2, right). In conclusion, we can make the assumption that flows ( $b_1$ ) and ( $b_2$ ) are equivalent to corotating flows observed in two oppositely rotating frames of frequencies  $+f_r$  and  $-f_r$  with  $|f_r| > \max(|f_1|, |f_2|)$ . This is well consistent with the fact that the single cell flows ( $b_1$ ) and ( $b_2$ ) exhibit global rotation in the outer shell  $R/2 \lesssim r \lesssim R$ . The stability of such solution is clearly enhanced by the concave curved blades that enforce ro-

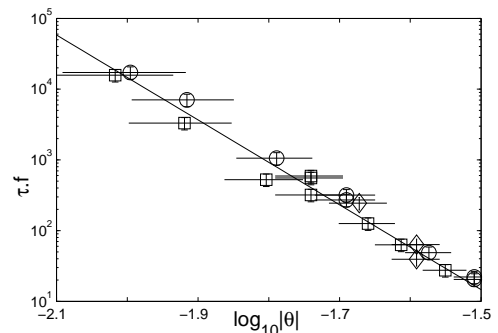


FIG. 6:  $\tau \cdot f$  vs.  $\theta$  for  $f = 4.16$  Hz/ $Re = 3.3 \times 10^5$  (○),  $f = 6$  Hz/ $Re = 4.7 \times 10^5$  (□) and  $f = 10$  Hz/ $Re = 7.9 \times 10^5$  (◇), fitted by a  $-6$  slope power law.

tation of the fluid near the outer cylinder.

Let's now consider how these three solution branches exchange their stability. First note that the bifurcation diagrams respect the  $\mathcal{R}_\pi$  symmetry:  $\theta \rightarrow -\theta$ ;  $\Delta K_p \rightarrow -\Delta K_p$ . The straight blades diagram (Fig. 4a) is continuous: from left to right two second order transitions  $(b_1) \leftrightarrow (s)$  and  $(s) \leftrightarrow (b_2)$  are observed as in small  $H/R$  systems [17]. On the contrary, the curved blades diagram (Fig. 4b) is strongly hysteretic. Addition of baffles (Fig. 4c) allows to remove a degeneracy: baffles drag disturb the outer cylinder boundary layer flow, thus lowering the relative stability of one-cell flows with respect to the two-cell flow. The large hysteresis cycle is split into two classical first-order bifurcations. This singular cycle can thus be viewed as the result of the collapse or collision of two first-order cycles. Similar cycles are encountered in conical [18] and delta-wing flows [3]. The memory effect —if the system is currently on  $(s)$ , both driving frequencies *must* have been increased in parallel— is thus essentially a consequence of the cycle structure.

In order to test the effect of turbulence on the stability of the observed flows, we lowered Reynolds number down to laminar using water/glycerol mixtures. While  $Re \lesssim 1000$ , no multiplicity is observed: the bifurcation diagram is similar to the straight-blade diagram of Fig. 4a. The cycle appears for  $Re$  between 1000 and 3000. The study is in progress and will be reported elsewhere. The high Reynolds behavior reported in this Letter is well established once  $Re \gtrsim 5000$ . Thus, multiplicity appears with turbulence and does not with laminar ( $Re \lesssim 110$ ) nor chaotic ( $Re \lesssim 1000$ ) flows. A possible explanation for the multiplicity could thus be the evolution of the outer cylinder boundary layer with  $Re$ .

Besides, the statistical nature of the transitions themselves is probably related to turbulent fluctuations. Let's first notice that the bifurcation studied here corresponds to exchange of stability between mean flows, these mean states being never realized at any given time. Is the bifurcation formalism exactly valid for our mean flows? On some aspects, our system behaves as a low-dimension dynamical system, as in the turbulent spiral transition observed in wide-aspect-ratio Taylor-Couette flow [19] or in the noise-induced Hopf bifurcation for a Duffing oscillator with multiplicative white noise [11]. However, suppose a non-linear amplitude equation could correctly describe the shape bifurcation diagram, it would probably not be able to catch the statistics of the transition from the two-cell state  $(s)$  to a one-cell state  $(b_1)$  or  $(b_2)$ . This transition shows a very peculiar statistics, with a very high critical exponent 6 (Fig. 6). It also strictly respects a forbidden-transition rule: the horizontal axis of the bifurcation diagram is never crossed, i.e.,  $(s) \rightarrow (b_2)$  [resp.  $(s) \rightarrow (b_1)$ ] is forbidden for  $\theta < 0$  [resp.  $\theta > 0$ ]. This observational fact could by itself justify the stability of the central point  $\theta = 0$ , which has to respect both rules. Furthermore, the non-crossing of the axis could be the

signature of multiplicative noise as suggested to account for small-scale turbulence [20].

The global bifurcation reported in this Letter presents a very unusual bifurcation diagram. Some features about the multistability have been searched among the mechanics of high-Reynolds-number flows, while some other simply involve the theory of non-linear bifurcations, possibly in the presence of noise. Among the transitions, the two-cell  $\rightarrow$  one-cell stability exchange plays a remarkable role, in presenting an original statistics of transition and putting the flow definitively in a state which breaks the  $\mathcal{R}_\pi$  symmetry of the system and does not allow the flow to restore statistically this symmetry when  $Re \rightarrow \infty$ .

We thank V. Padilla and C. Gasquet for efficient assistance in building and piloting the experiment, and B. Dubrulle, O. Dauchot and N. Leprovost for fruitful discussions.

---

\* Electronic address: arnaud.chiffaudel@cea.fr

- [1] O.R. Burrgraf & M.R. Foster, *J. Fluid Mech.* **80**, 685 (1977).
- [2] V. Shtern & F. Hussain, *Phys. Fluids A* **5**, 2183 (1993).
- [3] M.G. Goman, S.B. Zakharov & A.N. Khrabrov, *Sov. Phys. Dokl.* **30**, 323 (1985).
- [4] G. Schewe, *J. Fluid Mech.* **133**, 265 (1983).
- [5] V. Shtern & F. Hussain, *Annu. Rev. Fluid Mech.* **31**, 537 (1999).
- [6] G.K. Batchelor, *Quart. J. Mech. Appl. Math.* **4**, 29 (1951).
- [7] K. Stewartson, *Proc. Camb. Phil. Soc.* **49**, 333 (1953).
- [8] P.J. Zandbergen & G. Dijkstra, *Ann. Rev. Fluid Mech.* **19**, 465 (1987).
- [9] U. Frisch, *Turbulence - The legacy of A. N. Kolmogorov*, Cambridge University Press, New York, (1995).
- [10] S. Residori *et al.*, *Phys. Rev. Lett.* **88**, 024502 (2002).
- [11] K. Mallick & P. Marcq, *Eur. Phys. J. B* **31**, 553 (2003), *Eur. Phys. J. B* **36**, 119 (2003).
- [12] H.K. Moffatt, *Magnetic field generation in electrically conducting fluids*, Cambridge University Press, Cambridge, (1978).
- [13] O. Cadot, S. Douady & Y. Couder, *Phys. Fluids* **7**, 630 (1995).
- [14] R. Labbé, J.F. Pinton & S. Fauve, *J. Phys. II France* **6**, 1099 (1996).
- [15] T. von Kármán, *Zeit. Angew. Math. Mech.* **1**, 233 (1921).
- [16] We have experimentally shown [L. Marié, PhD. Thesis, University Paris 7, (2003)] that, when using inertial stirring bladed disks at high Reynolds number, the flat outer rotating cylinder may be rotated almost without any effect but developing a thin viscous boundary layer on it. The torque exerted through this layer can generally be neglected with respect to the impeller torques.
- [17] G. Dijkstra & G.J.F. van Heijst, *J. Fluid Mech.* **128**, 123 (1983).
- [18] V. Shtern & F. Hussain, *J. Fluid Mech.* **309**, 1 (1996).
- [19] A. Prigent *et al.*, *Phys. Rev. Lett.* **89**, 014501 (2002).
- [20] J.-P. Laval, B. Dubrulle & S. Nazarenko, *Phys. Fluids* **13**, 1995 (2001).